Inorganic-Organic Hybrid Nanoparticles with Carbonate-triggered Emission-Colour-Shift

Christian Ritschel[a], Lena J. Daumann[b], and Claus Feldmann[a*]

[a] MSc. Christian Ritschel, Prof. Dr. Claus Feldmann
Institut für Anorganische Chemie
Karlsruhe Institute of Technology (KIT)
Engesserstraße 15, D-76131 Karlsruhe (Germany)
Phone: (+)49-721-60842855
E-mail: claus.feldmann@kit.edu
Orcid-No: https://orcid.org/0000-0003-2426-9461

[b] Prof. Lena J. Daumann
Chair of Bioinorganic Chemistry
Heinrich-Heine-Universität Düsseldorf
Universitätsstraße 1, 40225 Düsseldorf (Germany)
E-mail: lena.daumann@hhu.de
Orcid-No: https://orcid.org/0000-0003-2197-136X

- Supporting Information -

Content

1. Analytical Equipment

Dynamic light scattering (DLS) measurements of the IOH-NPs were performed in polystyrene cuvettes (Brand, Germany) applying a Nanosizer ZS (Malvern Instruments, United Kingdom). Zeta potential measurements of the IOH-NPs were conducted using an automatic titrator MPT-2 attached to a Nanosizer ZS. Titrations were performed by addition of 0.1 M HCl or 0.1 M NaOH.

Scanning electron microscopy (SEM) was conducted with a Zeiss Supra 40 VP (Zeiss, Germany), equipped with a field-emission gun and a resolution of 1.3 nm (at 15 kV). Due to the organics content, the IOH-NPs are highly sensitive to the electron beam. To minimize the sample decomposition, examinations were performed at 1 to 5 kV. The samples were prepared by placing small droplets of diluted aqueous suspensions on a silica wafer.

X-ray powder diffraction (XRD) was conducted on a Stadi-P diffractometer (Stoe, Germany) with Ge-monochromatized Cu-Ka radiation. Dried IOH-NP samples were fixed between Scotch tape and acetate paper.

Fourier-transformed infrared (FT-IR) spectra were recorded on a Bruker Vertex 70 FT-IR spectrometer (Bruker, Germany) in the range of 4000-450 cm^{-1}. To this concern, 1 mg of the dried IOH-NP sample was mortared with 300 mg of dried KBr and pressed to a pellet that was analysed in transmission.

Thermogravimetry (TG) was performed with a STA409C device (Netzsch, Germany). All measurements were performed in air. The IOH-NP samples were dried in vacuo (10^{-3} mbar) prior to TG analysis and thereafter heated to 1200 °C with a heating rate of 5 K min^{-1} (20 mg, corundum crucibles).

Elemental analysis (EA) (C/H/N/S analysis) was performed via thermal combustion with an Elementar Vario Microcube device (Elementar, Germany) at a temperature of about 1100 °C.

Photoluminescence (PL) was recorded with a Horiba Jobin Yvon Spex Fluorolog 3 (Horiba Jobin Yvon, France) equipped with a 450 W Xe-lamp and double grating excitation and emission monochromators.

2. Characterization of TREN-1,2-HOPO

TREN-1,2-HOPO was prepared according to the literature.[S2] Its purity was examined via 1H-NMR spectra (Figure S1), using a Bruker AV600 NMR spectrometer: ^{1}H-NMR (600 MHz, d^{7}-DMF): δ / ppm = 9.46 (t, 3H), 7.48 (m, 3H), 6.69 – 6.71 (m, 6H), 4.00 (m, 6H), 3.76 (t, 6H).

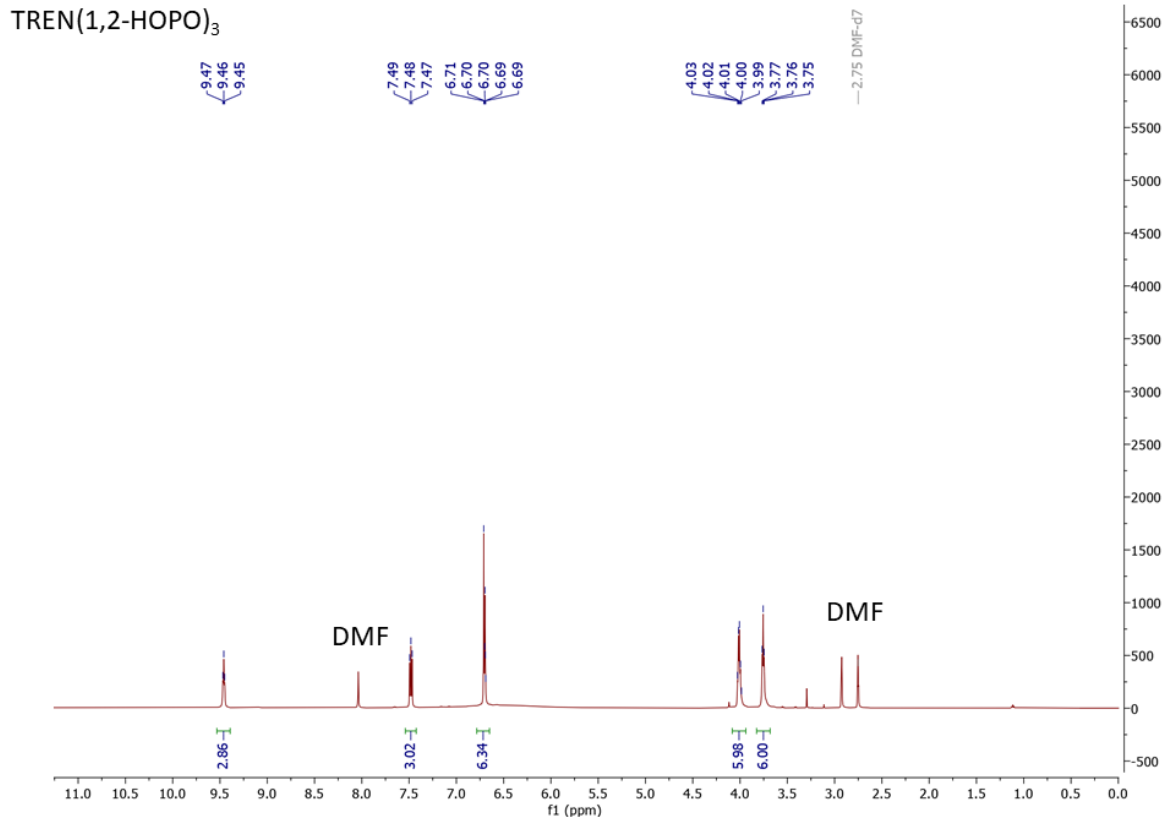

Figure S1. ^{1}H-NMR of TREN(1,2-HOPO)$_3$ in d^{7}-DMF.

3. Nanoparticle Characterization: $(Eu_4[PTC]_3)_{0.9}(Eu[TREN\text{-}1,2\text{-}HOPO])_{0.1}$

Scanning electron microscopy (SEM) images show rod-shaped nanoparticles with a length of about 60 nm and a diameter of about 5 nm. While a detailed SEM image is shown in the main paper (Figure 2b), SEM overview images are displayed in Figure S2. Based on a statistical evaluation of > 100 particles on SEM images, a mean rod length of 63±8 nm was determined (*main paper: Figure 2a*). In regard of the SEM images, it should be noticed that the rod-shaped nanoparticles show certain agglomeration on the sample holder when evaporating water as the polar liquid phase. Moreover, the nanoparticles are sensitive to the electron beam and show decomposition under electron bombardment with high-energy electrons.

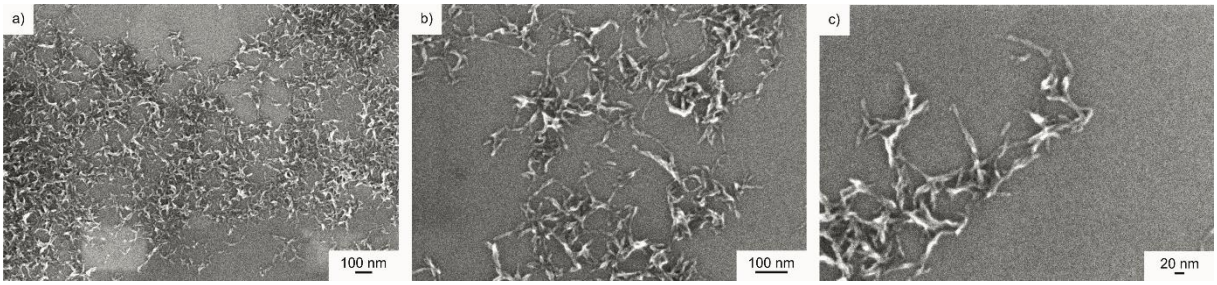

Figure S2. SEM overview images of $(Eu_4[PTC]_3)_{0.9}(Eu[TREN\text{-}1,2\text{-}HOPO])_{0.1}$ IOH-NPs at different levels of magnification.

Since diethylene glycol (DEG) was used to determine the particle size in suspension (*see main paper: Figure 2a*), SEM was also used to confirm shape and size of the $(Eu_4[PTC]_3)_{0.9}(Eu[TREN\text{-}1,2\text{-}HOPO])_{0.1}$ IOH-NPs after centrifugation from DEG (Figure S3). Taking the significance of the analysis into account, size and shape of the IOH-NPs are similar after separation from water and DEG.

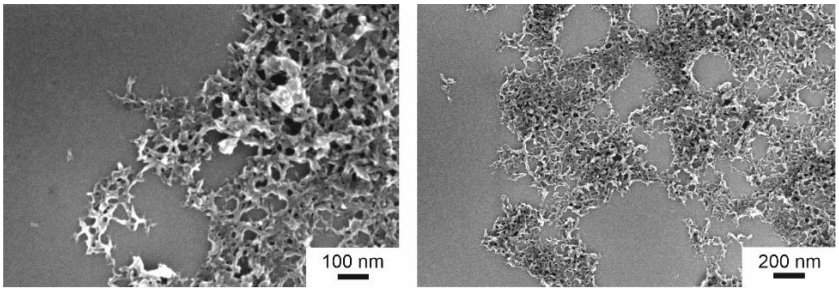

Figure S3. SEM overview images of $(Eu_4[PTC]_3)_{0.9}(Eu[TREN\text{-}1,2\text{-}HOPO])_{0.1}$ IOH-NPs after centrifugation from DEG.

The analysis of the chemical composition of the $(Eu_4[PTC]_3)_{0.9}(Eu[TREN\text{-}1,2\text{-}HOPO])_{0.1}$ is described in detail in the main paper. X-ray powder diffraction (XRD) indicates the IOH-NPs to be non-crystalline (Figure S4). According to FT-IR, all vibrations of the $(Eu_4[PTC]_3)_{0.9}(Eu[TREN\text{-}1,2\text{-}HOPO])_{0.1}$ IOH-NPs can be attributed to TREN-1,2-HOPO (specifically: ν(C=O): 1680 cm^{-1}, ν(C–N): 1207 cm^{-1}) and PTC (specifically: ν(C=O): 1595 cm^{-1}) (Figure S5).

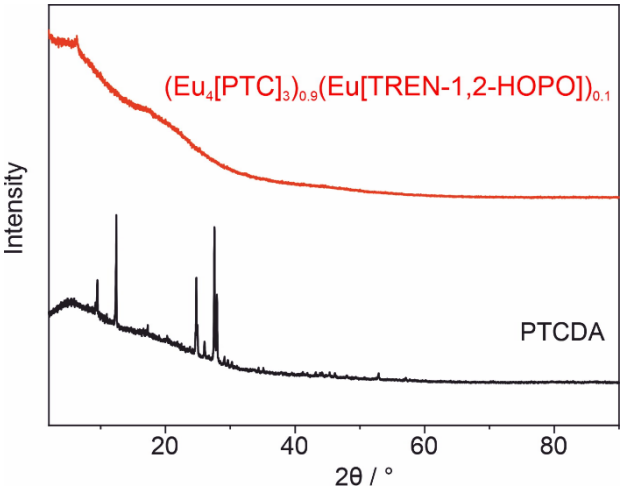

Figure S4. XRD of $(Eu_4[PTC]_3)_{0.9}(Eu[TREN\text{-}1,2\text{-}HOPO])_{0.1}$ IOH-NPs (PTCDA as a reference).

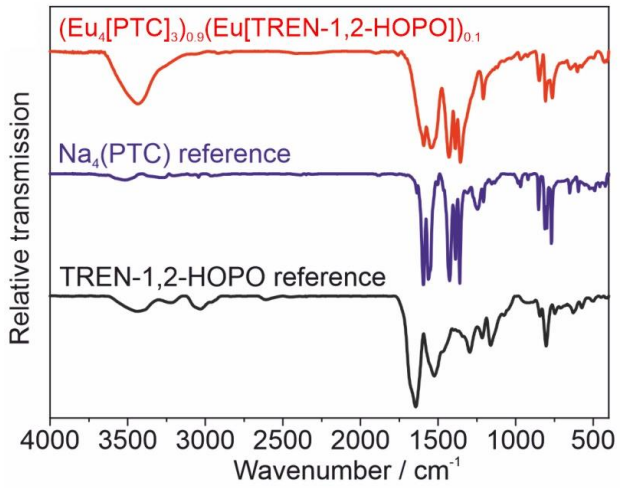

Figure S5. FT-IR spectrum of $(Eu_4[PTC]_3)_{0.9}(Eu[TREN\text{-}1,2\text{-}HOPO])_{0.1}$ IOH-NPs ($Na_4(PTC)$ and TREN-1,2-HOPO as references).

The main result from FT-IR spectra relates to the presence of the characteristic vibrations of TREN-1,2-HOPO and PTC in the IOH-NPs, which indicates the presence of these dyes in the $(Eu_4[PTC]_3)_{0.9}(Eu[TREN\text{-}1,2\text{-}HOPO])_{0.1}$ IOH-NPs. When comparing the vibrations of the pure dyes and of the IOH-NPs, two aspects are important (Tables S1,S2): (1) Due to the great number of dye molecules in a single IOH-NP and due to the fact that the IOH-NPs are amorphous without any periodic ordering, vibrations of the IOH-NPs become much broader than the vibrations of the pure dye compounds that are highly crystalline; (2) Due to the coordination of TREN-1,2-HOPO and PTC to the trivalent Eu^{3+} cation (instead of H^+ or Na^+ in the starting materials), certain vibrations show a shift of the wavenumber (specifically of the carboxylate

groups that are coordinated to Eu^{3+}). In fact, these shifts also proves the coordination of the respective dye anion to Eu^{3+}.

Table S1. Comparison of selected vibrations of the pure dye TREN-1,2-HOPO and the $(Eu_4[PTC]_3)_{0.9}(Eu[TREN\text{-}1,2\text{-}HOPO])_{0.1}$ IOH-NPs.

TREN-1,2-HOPO (cm^{-1})	$(Eu_4[PTC]_3)_{0.9}(Eu[TREN\text{-}1,2\text{-}HOPO])_{0.1}$ IOH-NPs (cm^{-1})
1680	1622
1643	1622 (partially superimposed by vibrations of PTC)
1522	1512 (partially superimposed by vibrations of PTC)
1296	1209 (partially superimposed by vibrations of PTC)

Table S2. Comparison of selected vibrations of the pure dye $Na_4(PTC)$ and the $(Eu_4[PTC]_3)_{0.9}(Eu[TREN\text{-}1,2\text{-}HOPO])_{0.1}$ IOH-NPs.

$Na_4(PTC)$ (cm^{-1})	$(Eu_4[PTC]_3)_{0.9}(Eu[TREN\text{-}1,2\text{-}HOPO])_{0.1}$ IOH-NPs (cm^{-1})
1595	1595
1562	1537
1425	1431
1389	1389
1360	1356
853	849
812	808
870	764

Furthermore, TG analysis shows the thermal decomposition of the $(Eu_4[PTC]_3)_{0.9}(Eu[TREN\text{-}1,2\text{-}HOPO])_{0.1}$ IOH-NPs with the release of adsorbed water as a first step (5.4 wt-%, < 200 °C) and a total organics combustion of 63.3 wt-% (up to 600 °C; corrected for the amount of adsorbed water to 67.1 wt-%) (Figure S6a). The thermal residue was identified by XRD to be Eu_2O_3, which indicates total-organics combustion at 1200 °C (Figure S6b).

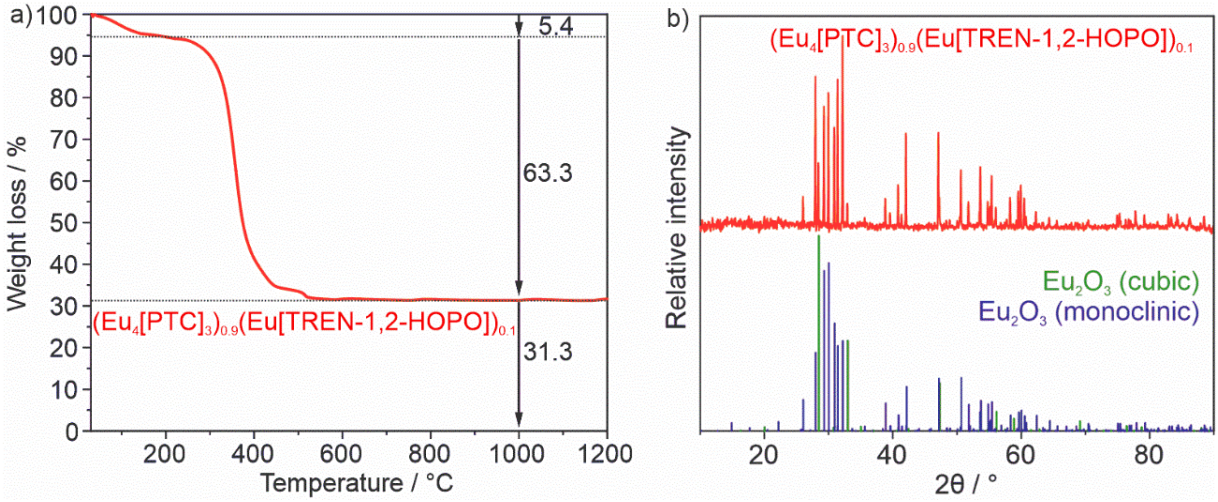

Figure S6. Chemical composition of $(Eu_4[PTC]_3)_{0.9}(Eu[TREN\text{-}1,2\text{-}HOPO])_{0.1}$ IOH-NPs: a) TG analysis, b) XRD of thermal remnant after TG analysis (cubic Eu_2O_3/ICSD-No. 194513 and monoclinic Eu_2O_3/ICSD-No. 8056 as references).

4. Nanoparticle Characterization: $Eu^{3+}{}_4[PTC]^{4-}{}_3$

For $Eu^{3+}{}_4[PTC]^{4-}{}_3$, EA reveals C/H/N contents of 42.4 wt-% C and 1.8 wt-% H. After correction for 6.3 % of adsorbed water (*see TG:* Figure S7a), these values were corrected to 45.4 wt-% C and 1.2 wt-% H. These values are in good agreement with the calculated values based on the composition $Eu^{3+}{}_4[PTC]^{4-}{}_3$ (46.0 wt-% C, 1.3 wt-% H). Furthermore, TG shows three-step decomposition with 6.3 wt-% of adsorbed water (< 200 °C) and 60.3 wt-% for total organics combustion (up to 600 °C) (Figure S7a). After correction for adsorbed water, the total organics combustions amounts to 64.5 wt-%, which is in accordance with the calculated value based on the composition $Eu^{3+}{}_4[PTC]^{4-}{}_3$ (62.6 wt-%). The thermal residue of TG analysis was identified via XRD as Eu_2O_3 (Figure S7b), so that the thermal decomposition of the $Eu^{3+}{}_4[PTC]^{4-}{}_3$ IOH-NPs can be ascribed to the following reaction:

$$Eu^{3+}{}_4[C_{24}H_8O_8]^{4-}{}_3 + 70.5\ O_2 \rightarrow 72\ CO_2 + 15\ H_2O + 2\ Eu_2O_3$$

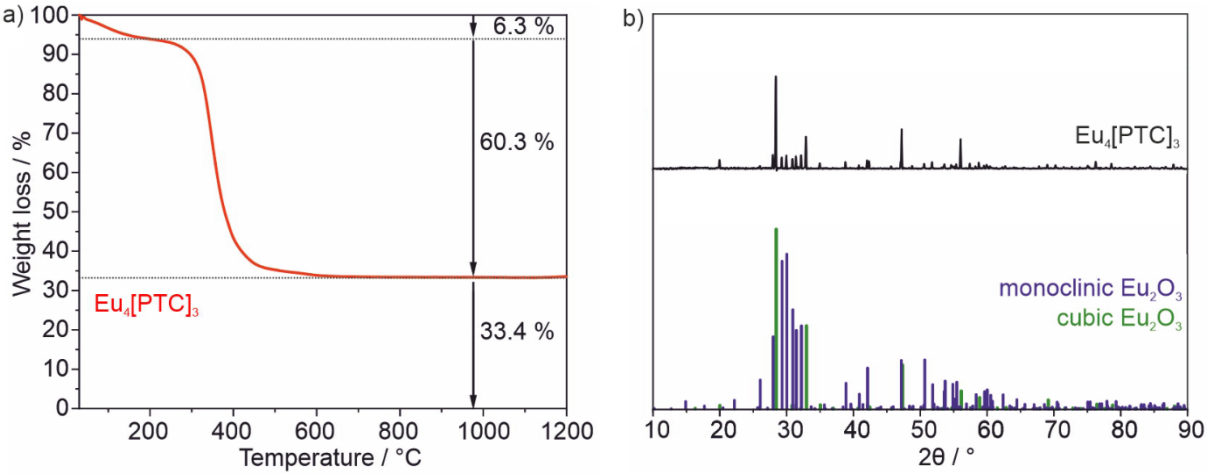

Figure S7. Chemical composition of $Eu^{3+}{}_4[PTC]^{4-}{}_3$ IOH-NPs: a) TG analysis, b) XRD of thermal remnant after TG analysis (cubic Eu_2O_3/ICSD-No. 194513 and monoclinic Eu_2O_3/ICSD-No. 8056 as references).

5. Luminescence Spectra

The luminescence characteristics of aqueous solutions of [Eu(TREN-1,2-HOPO)(H_2O)] (Figure S8) is very similar to the $(Eu_4[PTC]_3)_{0.9}(Eu[TREN\text{-}1,2\text{-}HOPO])_{0.1}$ IOH-NPs (*see main paper: Figure 3*). For [Eu(TREN-1,2-HOPO)(H_2O)] a quantum yield of 5-10 % and a decay of 222 µs were reported.[S1]

A solution of $Na_4(PTC)$ in water shows strong absorption at 280-380 nm and intense green emission at 480-620 nm (Figure S9).

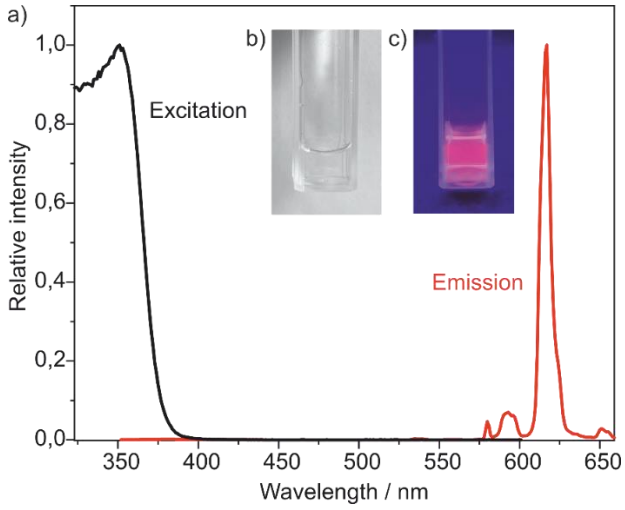

Figure S8. Luminescence of [Eu(TREN-1,2-HOPO)(H_2O)] (0.5 mg/mL, water): a) Excitation (λ_{em} = 616 nm) and emission (λ_{ex} = 337 nm) spectra; b) Photo of aqueous solution in daylight; c) Photo of aqueous suspension with excitation at 365 nm.

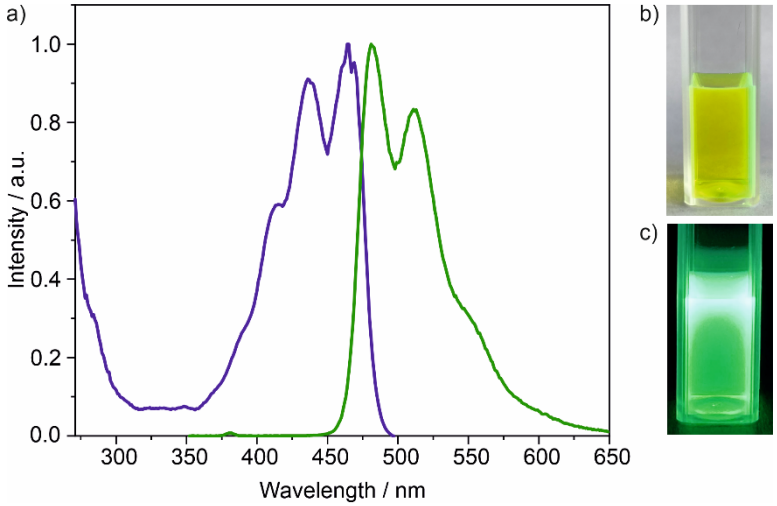

Figure S9. Luminescence of $Na_4(PTC)$ (in water): a) Excitation (λ_{em} = 512 nm) and emission (λ_{ex} = 337 nm) spectra; b) Photo of aqueous solution in daylight; c) Photo of aqueous solution with excitation at 365 nm.

The luminescence of the $(Eu^{3+}{}_4[PTC]^{4-}{}_3)_{0.9}(Eu^{3+}[TREN\text{-}1,2\text{-}HOPO]^{3-})_{0.1}$ IOH-NPs shows a clear correlation between the intensity of the PTC-driven green emission and the $NaHCO_3$ concentration as indicated by the respective emission spectra (*see main paper: Figure 4b*). With the carbonate-driven release of PTC from the IOH-NPs into the solution, the excitation of PTC increases as well (Figure S10).

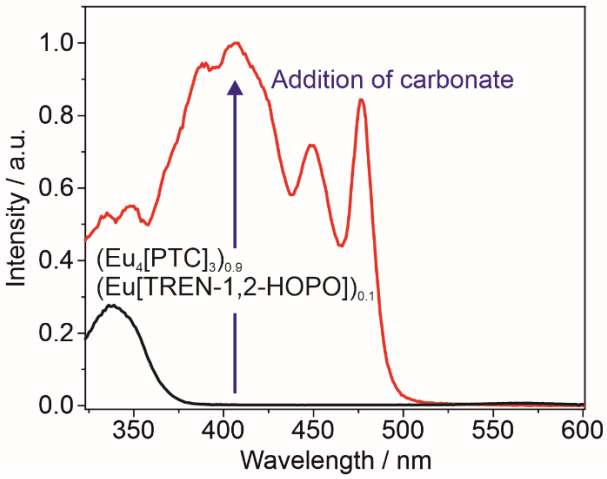

Figure S10. Excitation spectra of $(Eu^{3+}{}_4[PTC]^{4-}{}_3)_{0.9}(Eu^{3+}[TREN\text{-}1,2\text{-}HOPO]^{3-})_{0.1}$ IOH-NPs (0.25 mg/mL, water) prior and after the addition of carbonate (2 mM, water, λ_{em} = 616 nm).

The effect of the pH (without any carbonate addition) was evaluated for aqueous suspensions of $(Eu^{3+}{}_4[PTC]^{4-}{}_3)_{0.9}(Eu^{3+}[TREN\text{-}1,2\text{-}HOPO]^{3-})_{0.1}$ IOH-NPs (Figure S11). The pH was adjusted by addition of 0.01 M NaOH. At pH 5 to 7, the influence of the pH on the emission is

low (Figure S11a). Here, the linear correlation between emission and carbonate concentration also indicates the absence of any additional effect of the pH (*see main paper: Figure 4d*). Here, it should be noticed that the monochromator slit widths were identical for all emission spectra (3 nm; *main paper: Figure 4 and Figure S11*). At higher pH (> 7), however, the pH has an increasing effect on the emission intensity since OH^- also promotes a release of PTC (Figure S11b).

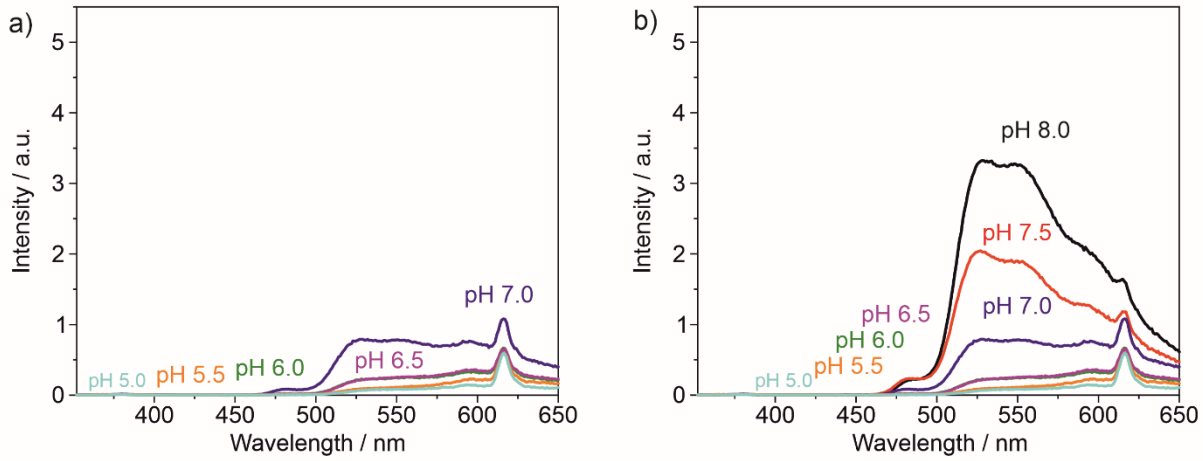

Figure S11. Emission spectra of $(Eu^{3+}{}_4[PTC]^{4-}{}_3)_{0.9}(Eu^{3+}[TREN\text{-}1,2\text{-}HOPO]^{3-})_{0.1}$ IOH-NPs (0.25 mg/mL, water) depending on the pH only and without any addition of carbonate (adjusted with 0.01 M NaOH; λ_{em} = 616 nm).

Beside the carbonate-initiated emission-colour shift, a similar effect was also observed after addition of phosphate (Figure S12).

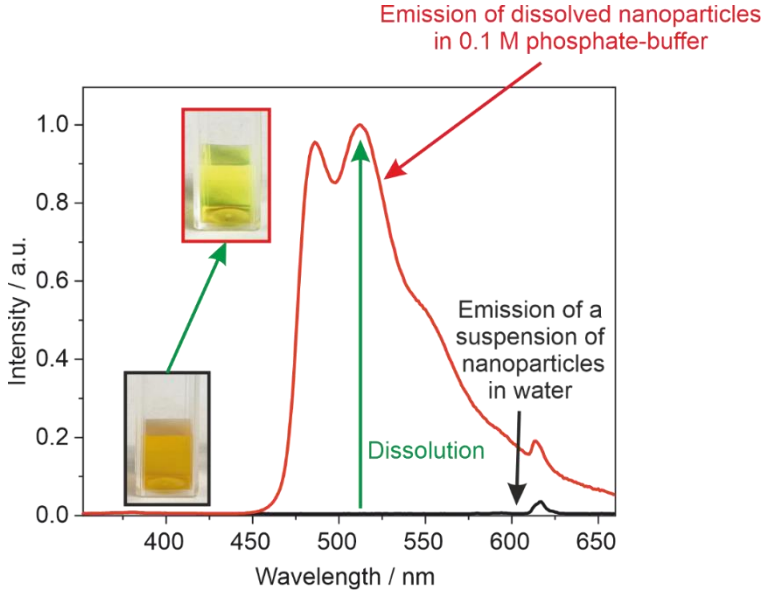

Figure S12. Emission of $(Eu_4[PTC]_3)_{0.9}(Eu[TREN\text{-}1,2\text{-}HOPO])_{0.1}$ IOH-NPs (0.5 mg/mL, water) after addition to NaH_2PO_4/Na_2HPO_4 buffer (0.1 M) (λ_{ex} = 337 nm).

References

S1 (a) P. S. Samuel and K. N. Raymond, *Acc. Chem. Res.*, 2009, **42**, 542. (b) C. J. Jocher, E. G. Moore, J. Xu, S. Avedano, M. Botta, S. Aime and K. N. Raymond, *Inorg. Chem.*, 2007, **46**, 9182-9191.

S2 J. Xu, D. G. Churchill, M. Botta and K. N. Raymond, *Inorg. Chem.*, 2004, **43**, 5492-5494.